Int. J. Mol. Sci. **2014**, *15*, 1-x manuscripts; doi:10.3390/ijms150x000x

OPEN ACCESS
International Journal of
Molecular Sciences
ISSN 1422-0067
www.mdpi.com/journal/ijms

Article

TupA: a tungstate binding protein in the periplasm of *Desulfovibrio alaskensis* G20.

Ana Rita Otrelo-Cardoso [1,†], Rashmi R Nair [1,†], Márcia A S Correia [1], Maria G Rivas [1,2,*] and Teresa Santos-Silva[1,*].

[1] REQUIMTE/CQFB, Departamento de Química, Faculdade de Ciências e Tecnologia, Universidade Nova de Lisboa, Portugal. E-Mails: a.cardoso@campus.fct.unl.pt (ARO-C); r.nair@fct.unl.pt (RRN); tsss@fct.unl.pt (TSS); mgabrielarivas@gmail.com (MGR)
[2] Departamento de Física, Facultad de Bioquímica y Ciencias Biológicas, Universidad Nacional del Litoral, Argentina.

† These authors contributed equally to this work.

* Author to whom correspondence should be addressed; E-Mail: tsss@fct.unl.pt; Tel +351-212948300 (ext: 10940) and m.rivas@fct.unl.pt; Tel +54-342-4575213 (ext: 30); Fax: + 54 342-4575221

Received: / Accepted: / Published:

Abstract: The TupABC system is involved in the cellular uptake of tungsten and belongs to the ABC (ATP binding cassette) type transporter systems. The TupA component is a periplasmic protein that binds tungstate anions, which are then transported through the membrane by the TupB component using ATP hydrolysis as energy source (reaction catalyzed by the ModC component).

We report the heterologous expression, purification, determination of affinity binding constants and crystallization of the *Desulfovibrio alaskensis* G20 TupA. The *tupA* gene (locus tag Dde_0234) was cloned in the pET46 Ek/LIC expression vector and the construct was used to transform BL21(DE3) cells. TupA expression and purification were optimized to a final yield of 10 mg of soluble pure protein per liter of culture medium. Native polyacrylamide gel electrophoresis was carried out showing that TupA binds both tungstate and molybdate ions and has no significant interaction with sulfate, phosphate or perchlorate. Quantitative analysis of metal binding by isothermal titration calorimetry was in agreement with these results but in addition shows that TupA has higher affinity to tungstate than molybdate.

The protein crystallizes in the presence of 30 % (w/v) polyethylene glycol 3350 using the hanging-drop vapour diffusion method. The crystals diffract X-rays beyond 1.4 Å resolution and belong to the $P2_1$ space group, with cell parameters *a*=52.25, *b*=42.50,

c=54.71 Å, β=95.43˚. A molecular replacement solution was found and the structure is currently under refinement.

Keywords: TupA, tungstate, metal transport, *Desulfovibrio*, sulfate reducing bacteria, protein-ligand interaction, isothermal titration calorimetry, X-ray crystallography.

1. Introduction

Molybdenum and tungsten are trace elements used by almost all forms of life. Since Mo and W atoms share several similar chemical characteristics, biological systems have to develop strategies to differentiate one metal from the other and avoid the incorrect metal insertion in active site of enzymes [1-2]. These metals enter the cell as soluble oxoanions, MoO_4^{2-} and WO_4^{2-}, through specific ATP-binding cassette (ABC) transporter systems. In prokaryotes these transport systems are divided in three different families: Mod, Wtp and Tup. All these systems are composed of a periplasmic protein (component A), a transmembrane pore forming protein (component B) and a cytoplasmic protein (component C) which hydrolyzes ATP to generate the energy necessary to transport the oxoanion into the cell cytoplasm [2-5]. The genes encoding the three components are organized in an operon (*mod*/*wtpABC*) or gene cluster (*tupABC*) regulated by a transcription factor known as ModE in case of the ModABC operon. Under excess of molybdate, ModE binds molybdate ions and suffers conformational changes and dimerizes. This metal–protein complex binds to a specific DNA sequence (located upstream of the *modABC* operon) and down-regulates the expression of proteins involved in molybdenum uptake [4, 6-8].

Under oxoanion starvation, the component A binds molybdate or tungstate and interacts with the component B to actively transport molybdate or tungstate from the periplasm to the cystoplasm [4]. Therefore the Mod/Wtp/TupABC transport system and more specifically the component A should constitute the first selection gate from which cells should differentiate between Mo and W. The basis for this selectivity is currently unknown. The periplasmic component of the Mod/Tup/WtpABC system differs not only in the primary sequence but also in the metal affinity and coordination chemistry of the molybdate/tungstate [2, 9-16]. Crystal structures of ModA have already been solved, showing a tetrahedral coordination with five conserved amino acids located at H-bond donating distance from the oxygen atoms of the oxanions [17-19]. Different from ModA, the tungstate binding protein WtpA binds tungstate in an distorted octahedral conformation with two carboxylate oxygens from conserved glutamate (Glu218) and aspartate (Asp160) residues (*Pyrococcus furiosus*, *Pf,* numbering), with several examples in the literature [20]. The oxoanion coordination in TupA protein has not yet been reported but it is known that the TTTS motif at the N-terminal amino acid sequence is a signature of this type of tungstate transporters. In this motif, the Thr9 and Ser11 (*Geobacter sulfurreducens, Gs,* numbering) are predicted to be interacting with the oxoanion through hydrogen bonds. In addition, a conserved threonine in the C-terminal domain, Thr124, is postulated to coordinate the oxoanion through hydrogen bonds [2]. The crystal structure of *Gs* TupA has been deposited in the Protein Data Bank (PDB code 3LR1) with a W^{6+} ion close to the TTTS motif. The binding mode of the ion is not clear and needs to be further scrutinized.

Desulfovibrio alaskensis G20 (*Da*G20) is a sulfate reducing bacterium (SRB) that obtains energy from sulfate reduction and produces sulfide, a highly toxic and corrosive metabolite [21]. SRB are the main responsible for a phenomenon known as microbiologically-influenced corrosion (MIC) with very relevant economic consequences in several industries, including the chemical, paper, power, marine and petroleum industry [22-24]. Molybdate can be used to control the SRB growth mainly by inhibition of ATP-sulfurylase, a key enzyme in sulfate activation [25-27]. In addition, we have observed that high molybdate concentration in cultures of *Da*G20 affect the expression of proteins involved in energy metabolism, ion transport, cell cycle, aminoacid, purines, pyrimidines, nucleosides and nucleotides biosynthesis and other cellular mechanisms. Regarding the proteins involved in ion transport, we found that not only the periplasmic protein involved in molybdate transport (ModA) but also the protein involved in tungstate transport (TupA) are down-regulated under these stress conditions (Nair R.R., *manuscript under review*).

Despite the presence of several relevant Mo and W containing enzymes in the *Desulfovibrio* metabolism, there are no reports about molybdate/tungstate transport systems in this organism. Genome analysis shows that it codifies both molybdate and tungstate transporters. The tungstate transport system corresponds to the Tup kind of transporters. Analysis of the primary sequence of the *Da*G20 TupA contains all the conserved residues putatively involved in the oxoanion coordination [1] (Figure 3).

Here we report the expression, purification, determination of affinity binding constants and crystallization of the *Da*G20 TupA protein. The high resolution structure (up to 1.4 Å resolution) will provide useful information about the coordination geometry of the oxoanion to the protein. In addition, the expression system and purification protocol described are useful to construct mutants that will make a relevant contribution to the knowledge of the selectivity mechanisms that allow to the cell differentiate between Mo and W.

2. Results and Discussion

2.1. Cloning and purification of TupA protein

The *tupA* gene (Dde_0234) was cloned into the pET-46 Ek/LIC vector using the Ek-LIC cloning system (Novagen) and the protein was expressed in BL21(DE3) cells. The expression level of TupA and the ratio TupA/contaminants were evaluated by SDS-PAGE at different induction times (3 h, 5 h and overnight) and 3 h induction was considered the optimum condition for TupA production in BL21(DE3) cells. SDS-PAGE showed that TupA is present in both soluble and insoluble fraction (data not shown). Since the amount of TupA in the soluble fraction was considered enough to perform the studies here described, we proceed to isolate the protein from this fraction. As explained in the materials and methods section, TupA purification protocol includes two steps, an anionic exchange and a size exclusion chromatography. TupA elutes from the anionic exchange resin at approximately 200 mM Tris-HCl (pH 7.6) which is in agreement with the isoelectric point calculated for the protein (pI 5.69, ProtParam tool [28]). The degree of purity after each purification step was evaluated by SDS-PAGE (Figure 1). According to the protein sequence the molecular weight of the recombinant protein

should be approximately 29 kDa. The purification yield was calculated to be approximately 10 mg of soluble protein per liter of cell culture.

Figure 1. SDS-PAGE stained with Coomassie blue of 1) Molecular weight markers (Biorad; from top: 100, 75, 50, 37, 25, 20, 15 and 10 kDa), 2) Soluble protein fraction, 3) TupA fraction after anionic exchange chromatography and 4) TupA fraction after molecular exclusion chromatography (approximately 15 µg of pure protein).

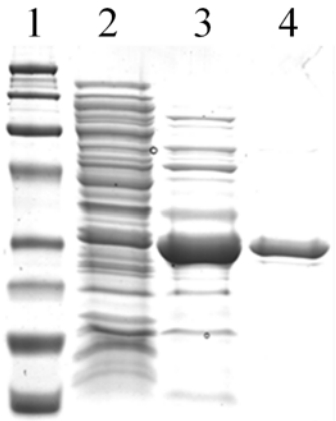

2.2. UV-visible spectrum and protein sequence.

The UV-visible spectrum of the as-isolated TupA protein is shown in Figure 2. The maximum observed at 280 nm is due to the six Tyr residues present in the primary structure whereas the shoulder at 288 nm is probably derived from the four Trp residues (Figure 3, Dde_0234).

The extinction coefficient of TupA at 280 nm (29700 ± 700 $mM^{-1}cm^{-1}$) was found to be in good agreement with that deduced from the amino acid sequence of the pure protein (30440 $mM^{-1}cm^{-1}$).

Multiple sequence alignment of TupA proteins shows that the *Da*G20 TupA contains the TTTS motif at the N-terminal region which is the typical signature of this kind of tungstate transporters. The amino acids suggested to form hydrogen bonds with the oxoanion are Thr–124, Thr–9 and Ser–11 (the last two residues from the TTTS motif, *G. sulfurreducens* numbering). In addition, another conserved and a positively charged Arg–118 is highly conserved not only in the *Da*G20 TupA but also in TupA from different *Desulfovibrio* species. This residue is proposed as the structural element conferring the high selectivity of the TupA proteins (Figure 3).

Figure 2. UV-visible spectrum of as isolated TupA protein (0.020 µM protein in 50 mM Tris-HCl pH 7.6).

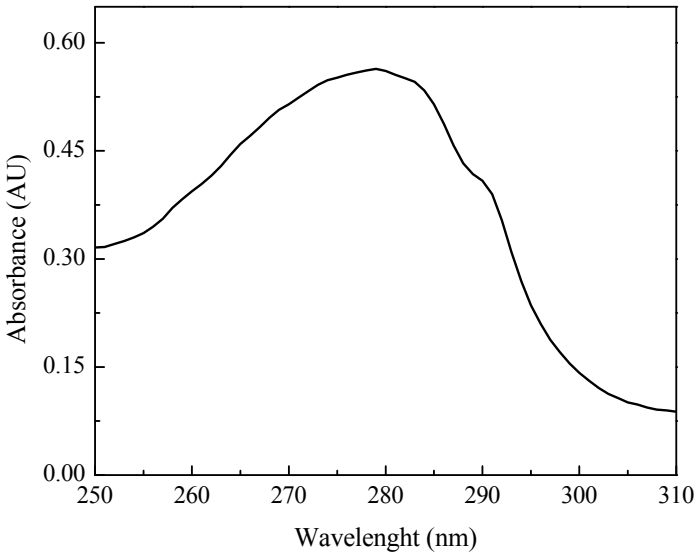

Figure 3. Multiple sequence alignment of TupA proteins performed with CLUSTALW [29]. Dde_0234, *Desulfovibrio alaskensis* G20; DVU0745, *Desulfovibrio vulgaris* Hildenborough; Dde_2876, *Desulfovibrio salexigens*; Cj1540, *Campilobacter jejuni* strain NCTC 11168; Dde_1778, *Desulfovibrio desulfuricans* ATCC 27774; GSU2700, *Geobacter sulfurreducens*. Residues putatively involved in coordination of tungstate are highlighted in black. Symbols: (*) identity, (:) strongly similar, and (.) weakly similar.

```
                        10        20        30        40        50        60        70        80        90       100
                         |         |         |         |         |         |         |         |         |         |
Dde_0234     -MR--KLLLVLALVMSLTG-VAYAEAPVLMMATTTSTDNTGLLDDLAPQFTKDTGIELRWTAVGTGKALKMGENCDVDILLVHAPAAEKAFVDAGFGTAR
DVU0745      -MR--RLLFLTCLLAAVISSSAFAADKVLMMATTTSTADTGLLDYLAPLFQKDTGIEVKWTAVGTGKALEMGKNCDVDVLLVHSPSAEAKFIEAGSGIER
Desal_2876   -MKKLKVLLLTFALVSLLVAPGLVKAETLMMATTTSTDNTGLLDELAPKFQKETGIELKWTAVGTGKALKMGQNCDVDVLMVHAPAAEKKNVDMGALKDR
Cj1540       -MK----KIISLALALALS----ASAAELKMATTTSTDNTGLLDALKPLYEKESGNTLKWVAVGTGAALKMGEDCNADVLFVHSPKAEKEFMKKGFGVDR
Ddes_1778    MFRMSRLFLAACVMGLLALAPVARAADVLMMATTTSTQDSGLLEYLEPFFKKETGMELKWVAVGTGKALEIAKNCDADVLLVHAPAAELEFIKAGHGTDR
GSU2700      -MKMYR-SFAATLVALLMLVTVAGAEERLKMSTTTSTQDSGLLKVLLPPFEKKNNVKVDVIAVGTGQALKLGEAGDVDVVFVHARKLEDKFVADGFGVNR
              ::     :    :             * *:***** ::***. * * : *...  :   ***** **::.:  :.*:::**:   *   :  *    *


                       110       120       130       140       150       160       170       180       190       200
                         |         |         |         |         |         |         |         |         |         |
Dde_0234     TQLMYNDFVIIGPAADPAGVK-GMTVAAALGRIAADNAVFVSRGDNSGTHKMEKSLWKQIEGSSPEKEAWYVQTGQGMLRTINVAAEKGGYTMTDRGTYI
DVU0745      TQLMYNDFVLVGPVADAAKAA-GKSVDAALKGIAAAKSPFLSRGDKSGTHNLEVKLWEKS-GMAPDKESWYVSTGQGMLRTIAMAAEMGGYTVTDRGTWI
Desal_2876   REVMYNDFVIIGPDSDPAGIK-GLPVVQAMKAVADAKAAFVSRGDNSGTNKKEISLWKVAGMAVPDKAEWYIQTGQGMIKSITVAEERDAYIMTDRGTYI
Cj1540       TPVMYNDFIIIADKSLASKFK-GKNLKESLELIKNEKLTFISRGDKSGTDNKEKSLWKNL-GGVPEKQSWYQQSGQGMLASIKIAEEKKGVILTDRGTYI
Ddes_1778    RQIMYNDFVIVGPKADPAKIA-GKSSAEALGRILKSKAGFVSRGDQSGTHKAEQKLWQQA-GITPDKDPAYFSAGQGMMATLNMAAEKKAYALTDRGTWI
GSU2700      KDVMYNDFVIVGPKNDPAGIAKAKTAAEALKLLATKGATFISRGDKSGTHTKELDLWKSA--GVDPKGNWYVEAGQGMGPVITMATERRAYTLTDRGTYN
               :*****:::.    .:    .     ::  :      *:****:***.. * .**:        *   * .:****   : :* *  .  :*****:


                       210       220       230       240       250       260       270       280
                         |         |         |         |         |         |         |         |
Dde_0234     KYEASMDGNPPLKILVEGDKILFNQYSAIPVNPAHCPKVKKDLADKFVNWMASPATQKTIGDFKLMGKALFTPNAE----
DVU0745      KYESTLNGAPVLKIIVEGDKSLLNQYSGIVVNPAQCPKVKADLAREYIKWMASPAGQKYIGDFLVSGKPLFTPNAGK---
Desal_2876   KYSANKNGSPELKVLVEGDKSLFNQYSVLAVNPANCKNAKYELATKFSEWMASPSTQKAIGDFKLLGKKLFIPNAK----
Cj1540       KYEANEKGKPNLVIVNEGDDSLKNFYSVIATNPKHCKNVNYTEASKFIKWVTSDKTLNFIADFKLLNKPLFVIDAKTRKD
Ddes_1778    TFADKAGADNPLAIAMEGDTALFNQYSVITVNPDRCPKVDKALAQKFEDWWVSPSTQQKIADYKLKGKQLFFPNAGK---
GSU2700      AFKG---AKTDLVILFQGEKGLFNPYGIMAVNPKKFPHVKYDLAMKLIDYVTGPEGLKIISDYKAHGEPVFFIYKK----
              :     .   * :  :*:  * * *. : .** .  :..   * :  .: ..    : *.*:   .: :*
```

2.3. Metal binding assays

Sequence analysis suggests that *Da*G20 TupA is a tungstate-binding protein that is able to bind tungstate and molybdate ions. To test the affinity and specificity of TupA to different anions, native polyacrylamide gel electrophoresis of samples pre-incubated with different oxoanions (MoO_4^{2-}, WO_4^{2-},

SO_4^{2-}, PO_4^{3-}, and ClO_4^-) was carried out similar to that described in reference [8]. The samples were submitted to gel filtration column prior to loading on native polyacrylamide gel in order to separate the unbound ions and ensure that differences in mobility were only due to the binding of anions to the protein. As seen in Figure 4, TupA showed a significant mobility shift upon binding to tungstate and molybdate, but not with the other anions. Both molybdate and tungstate induced similar shifts in the mobility of TupA and incubation with higher concentrations of anions (100 fold) had no visual impact. Quantitative studies of molybdate and tungstate binding was then performed using ITC.

Figure 4. Ligand dependent mobility shift assays for TupA protein (14 μM) in the presence of different oxoanions (10 fold excess). Lane 1: TupA; Lane 2: TupA + MoO_4^{2-}; Lane 3: TupA + WO_4^{2-}; Lane 4: TupA + SO_4^{2-}; Lane 5: TupA + PO_4^{3-}; Lane 6: TupA + ClO_4^-.

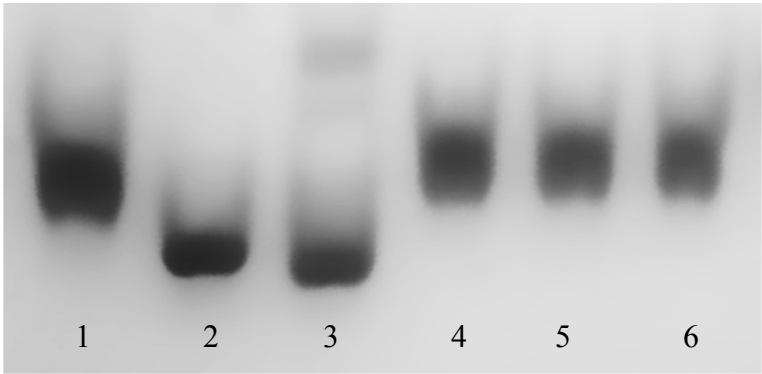

2.4. Isothermal titration calorimetry (ITC).

ITC has been proven to be a sensitive method to determine affinity constants for tungstate- and molybdate-binding proteins, TupA and ModA, in the nanomolar and subnanomolar ranges [10, 12, 16]. It has the advantage that nearly all interactions give rise to a heat change, which can be monitored with a high-sensitivity calorimeter, and the binding enthalpy (ΔH_{obs}) and dissociation constant can be derived. The observed behavior of TupA is consistent with an exothermic process at this temperature (30°C), with a single binding site model of binding. However the thigh nature of these bindings precluded an accurate fit to determine the K_D values. Displacement titrations were done to obtain the correct affinities. The K_D value of a displacement titration in combination with the K_D value for the inhibiting ligand in the absence of strong binding ligand can be used to calculate the actual K_D for the strong binding ligand (equation 1, see section 3.6).

ITC of TupA showed that the protein exothermically binds tungstate and molybdate with a stoichiometry of 1 mole oxoanion per mole of protein, as deduced from the heat release upon addition of tungstate or molybdate to the protein solution (Figure 5B). Direct titration of sodium molybdate against TupA produced an exothermic binding isotherm with a K_D value of 6.1 ± 0.9 nM. The value of

211 ΔH_{obs} (~6.6 kcal/mole of injectant) is also significantly less favorable, when compared with the
212 tungstate binding. In contrast, the binding of tungstate to TupA is much more exothermic (Figure 5A;
213 Table 1) with ΔH_{obs} being increased to ~14 kcal/mole of injectant (Table 1). The extremely high
214 affinity of the protein for tungstate resulted in a very steep binding curve, which hampers the
215 determination of K_D. In order to overcome this problem and determine a K_D value for tungstate, a
216 binding competition strategy was adopted. A displacement titration of the molybdate-saturated protein
217 with tungstate clearly showed that the protein favors the binding of tungstate, even when the binding
218 site is occupied with a molybdate molecule. The apparent binding constant depends on the
219 concentration of free molybdate, which was 0.5 mM and therefore K_D for tungstate when the protein
220 is saturated with molybdate was determined to be 6.30 ± 0.02 pM (Figure 5C, Table 1). The
221 displacement titration and the extremely low K_D value for tungstate indicate the latter should be the
222 physiological substrate for TupA, as expected. The results obtained are in good agreement with those
223 obtained for tungstate binding proteins from *Campilobacter jejuni* [12], *P. furiosus* [10] and is
224 approximately 1000 times higher than the K_D value obtained for the *E. acidaminophilum* TupA [11].
225

226 **Table 1 -** Data for ITC analysis of oxyanion binding to TupA and ModA proteins at 30 ºC.

	Ligand	n	K_A (M^{-1})	K_D (nM)	ΔH (kcal mol^{-1})
TupA	WO_4^{2-}	0.842 ± 0.001	$2x10^9 \pm 2x10^9$	0.5 ± 0.4	-13.500 ± 0.005
	MoO_4^{2-}	0.868 ± 0.002	$16x10^7 \pm 2x10^7$	6.1 ± 0.9	-6.600 ± 0.003
TupA + 0.5mM MoO_4^{2-}	WO_4^{2-}	0.845 ± 0.003	$1600x10^8 \pm 6x10^8$	$6.30x10^{-3} \pm 0.02x10^{-3}$	-14.60 ± 0.04
TupA + 0.5mM WO_4^{2-}	MoO_4^{2-}	No displacement			

227 in each case 10 mM protein was used for the titrations.
228 n = measured stoichiometry of binding.
229

230

Figure 5 - Isothermal titration calorimetry of ligand binding to TupA. 10 µM of TupA was titrated with injections of 100 µM tungstate (A) and 100 µM molybdate (B). (C) Displacement titration of 10 µM TupA incubated with 0.5 nM molybdate, with injections of 100 µM tungstate. Data were fitted with ORIGIN software. The raw ITC data are shown in the top graphs.

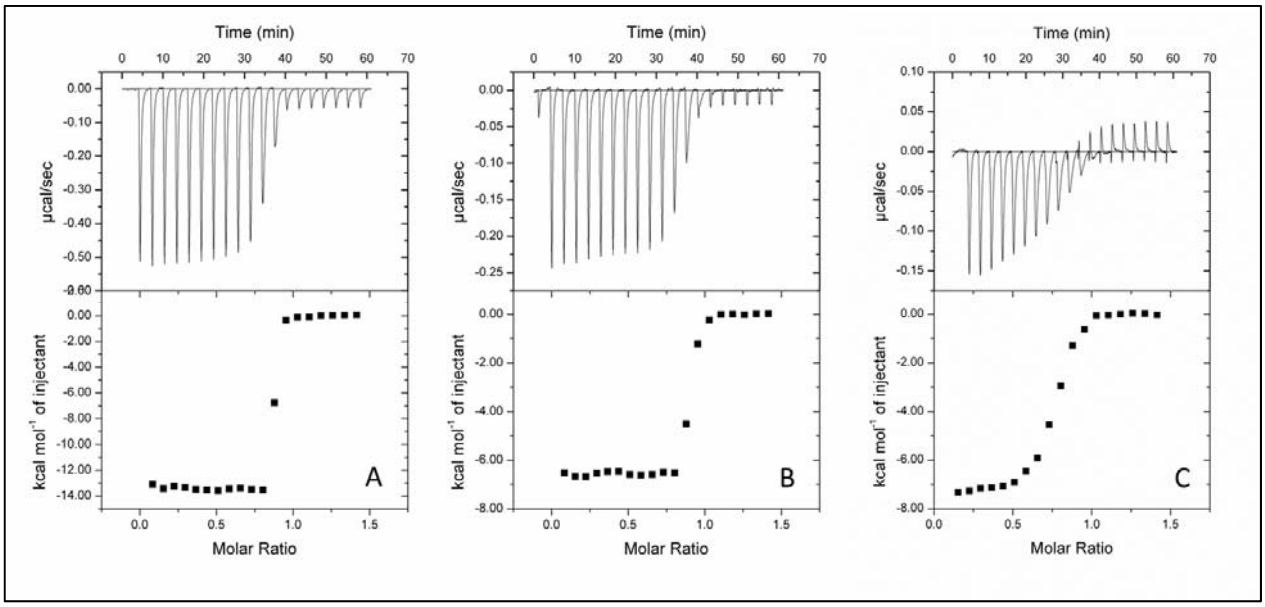

2.5. Crystallization and data processing

To crystallize TupA from *Da*G20 several commercial screens were tested in a 96 well plate using the sitting drop/vapour diffusion method. Plate shaped crystals appeared four days after crystallization setup when using a solution of 0.2 M magnesium chloride, 0.1 M Hepes pH 7.5 and 30 % (w/v) polyethylene glycol 3350 as precipitating agent (Figure 6).

The scale-up optimization was achieved by varying protein:precipitant proportion in the crystallization drop and crystals diffracting up to 1.43 Å resolution were obtained (data collection statistics are presented in Table 2). The crystals belong to the space group $P2_1$ and the Matthews coefficient calculation (2.09 $Å^3$ Da^{-1}) suggests the presence of one molecule of TupA per asymmetric unit and a solvent content of 40.84%. The L test for twinning indicates that these correspond to untwined crystals [30] .

Figure 6. TupA crystal grown in 0.2 M magnesium chloride, 0.1 M Hepes pH 7.5 and 30 % (w/v) polyethylene glycol 3350 solution. Each unit in the scale bar correspond to 0.1 mm.

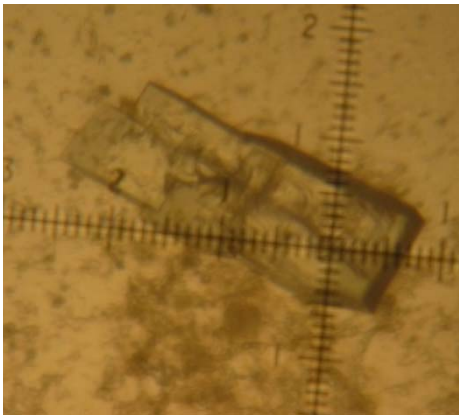

Table 2. Data-collection and processing statistics for TupA crystal. Values in parentheses correspond to the highest resolution shell.

$* R_{merge} = \sum_{hkl}\sum_i |I_i(hkl) - \langle I(hkl)\rangle| / \sum_{hkl}\sum_i I_i(hkl)$ $+ R_{pim} = \sum_{hkl}\left[\frac{1}{N-1}\right] 1/2 \sum_i |I_i(hkl) - \langle I(hkl)\rangle| / \sum_{hkl}\sum_i I_i(hkl)$

$\S\ R_{meas} = \sum_{hkl}\left[\frac{N}{N-1}\right] 1/2 \sum_i |I_i(hkl) - \langle I(hkl)\rangle| / \sum_{hkl}\sum_i I_i(hkl)$

Data collection parameters	
X-ray Source	ID23-1 (ESRF, Grenoble)
Detector	PILATUS 6M-F
Wavelength (Å)	0.954
Processing statistics	
Unit-cell parameters (Å, °)	a=52.25 b=42.50 c=54.71 β=95.43
Space group	P 1 2 1 1
Molecules per AU	1
Matthews coefficient (Å^3/Da)	2.09
Mosaicity (°)	0.22
Resolution range (Å)	42.50-1.43 (1.45-1.43)
<I/σI>	10.3 (2.1)
R_{merge} (%)*	4.1 (33.5)
R_{pim} (%)$^+$	2.7 (23.4)
R_{meas} (%)§	5.0 (4.1)
Multiplicity	3.0 (2.8)
No. of observed reflections	132115 (6040)
No. of unique reflections	43950 (2151)
Completeness (%)	99.1 (98.8)

2.6. Structure determination

To solve the structure of TupA, sequence alignments were performed in order to find the best homologous models that could lead to good initial phases obtained by molecular replacement (MR). The available structures deposited in the PDB, from the three families of transporters ModA, WtpA and TupA, have low sequence identity but a high degree of three-dimensional homology, with very

few structural differences. Structure determination was performed with PHASER [31] using as molecular models: a conserved functionally unknown protein from *Vibrio parahaemolyticus* RIMD 2210633 (PBD code 3MUQ) and the *Gs* TupA (PDB code 3LR1). In the first attempts to solve the phase problem, the two homology models were superposed and the non-conserved aminoacids were pruned in order to facilitate the rotational and translational searches. Nevertheless, a MR solution could only be obtained when searching for small sections of the protein separately: section I, from residues 1 to 81; section II from residues 82 to 188 and finally section III, from residues 189 to 236. This procedure is commonly used for large, multi-domain or oligomeric proteins, where a high degree of flexibility is expected between the different domains/subunits. In the present case, it suggests that *Da*G20 TupA is also a flexible protein that can adopt multiple conformations. The protein crystal structure is currently under refinement and details of the putative tungstate/molybdate binding site are going to be inferred.

3. Experimental Section

3.1. Bacterial strains and plasmids

The *Da*G20 cells were grown in 100 mL rubber stropped flasks containing 90 mL of medium C from Postgate [32] at 37 °C under anaerobic conditions. Media preparation includes oxygen removal by boiling and bubbling with pure argon for 30 min and sterilization at 121 °C at 20 psi for 20 minutes. The information on the bacteria strain, plasmid and primers used in this study are given in detail in Table 3.

Table 3. Bacterial strains and plasmids used in this study.

Strain/Plasmid/primer	Properties/sequence	Source/Reference
*Da*G20	Spontaneously nalidixic acid resistant derivative of G100A, isolated from the production fluids of offshore oil fields in Alaska.	Feio, M.J. [21], Hauser, L.J. [33] and Wall, J.D. [34].
pET-46 Ek/LIC vector	*E. coli* cloning vector plasmid	Novagen
NovaBlue GigaSingles cells	*endA1 hsdR17* (rK12$^-$ mK12$^+$) *supE44 thi-1 recA1 gyrA96 relA1 lac* [F'p*roA*$^+$*B*$^+$ *lacI*^{q}*ZΔM15*::Tn*10*(Tc^R)]	Novagen
E coli BL21(DE3)	*F*$^-$ *ompT gal dcm lon hsdSB(rB*$^-$ *mB*$^-$*) λ(DE3 [lacI lacUV5-T7 gene 1 ind1 sam7 nin5])*	Studier, F.W.[35]
TupA_LIC_Fwd (sense)	GACGACGACAAGATGCTGGAAGTTCTGTT CCAGGGGCCCGAAGCACCGGTTCTTATG	This work
TupA_LIC_Rev (antisense)	GAGGAGAAGCCCGGTTATTCGGCGTTGGG GGT	This work

284 *3.2. Cloning of tupA gene and protein expression optimization*

285 The *tupA* gene (locus tag Dde_0234) was amplified from *Da*G20 cells using the primers included in
286 Table 3. DNA template was obtained from *Da*G20 cells grown until the stationary phase. Briefly, 1
287 mL of the cell culture was centrifuged and the pellet was resuspended in 30 µL of sterile deionized
288 water. This suspension was boiled for 5 min in a boiling water bath and then centrifuged at 14000 rpm
289 for 2 min. A volume of 2 µL of the supernatant was used as DNA template. The amplification reaction
290 was carried out using FideliTaq™ DNA polymerase (Expand High Fidelity PCR System, Roche)
291 following the manufacturer's instructions. The PCR program was as follows: initial denaturation step
292 for 2 min at 92 °C followed by 25 cycles of 92 °C for 30 s, 55 °C for 30 s and 68 °C for 1 min and final
293 extension of 68 °C for 5 min. The amplicon (approximately 800 bp) was purified using the QIAquick
294 extraction kit (Qiagen) and quantified by the UV-visible spectrum. The insert (240 ng) was cloned in
295 the pET-46 Ek-LIC vector using the LIC cloning system (Novagen) following the manufacturer's
296 instructions. NovaBlue GigaSingles competent cells (Novagen) were transformed with the pET46-
297 tupA expression vector and the plasmid was isolated from a single colony using the NZY-Tech
298 Miniprep kit. The recombinant plasmids were sequenced using an ABI3700 DNA analyzer
299 (Perkin/Elmer/Applied Biosystems, Stabvida, Caparica, Portugal). The sequences were analyzed and
300 aligned using the online tool BLASTp [36] and CLUSTAL-W [37].
301 BL21(DE3) cells were transformed with the pET46-tupA expression vector and the protein production
302 was evaluated at different concentrations of IPTG (0, 0.2, 0.5 and 1.0 mM) and induction time (3 h, 5 h
303 and overnight). To test whether TupA is produced as a soluble protein the BugBuster reagent
304 (Novagen) was used as per protocol.

305 *3.3. Protein expression and purification*

306 *E. coli* BL21(DE3) cells containing the pET46-tupA were cultured in sterile Luria Bertanii medium
307 containing ampicillin (100 µg/mL) at 220 rpm and 37 ºC. When the OD_{600} reached 0.4 AU, cells were
308 induced with 0.1 mM IPTG during 3 h at room temperature. The cells were collected by centrifugation
309 at 7000 rpm for 15 min, washed in 5 mM Tris-HCl buffer, centrifuged at 7000 rpm for 15 min and
310 resuspended again in 5 mM Tris-HCl buffer containing DNase (5 µg/ml) at a ratio of 2 g cells/ml. The
311 cell suspension was freeze and thawed thrice before disrupting the cells on a French press cell at 150
312 psi. The crude extract was centrifuged at 9000 rpm for 30 min, ultracentrifuged (Beckman Coulter
313 Optima™ LE-80K) at 45000 for 45 min × g and the soluble fraction was filtered through a 0.45 µm
314 membrane. Although the pET-46 Ek/LIC expression vector encoded a six-histidine tag at the N-
315 terminal sequence, attempts to purify TupA using Immobilized-metal affinity chromatography (IMAC)
316 failed to bind the protein to the resin. Hence the strategy to purify TupA was changed to the protocol
317 followed described. The first purification step involved the loading of the soluble extract into a DEAE
318 Sepharose Fast Flow (GE-Healthcare) resin equilibrated with 3 column volumes (CV) of 5 mM Tris-
319 HCl (equilibration buffer). After protein loading, the resin was washed with equilibration buffer to
320 remove the unbound proteins and TupA was eluted using a gradient from 5 mM to 500 mM Tris-HCl
321 buffer in 8 CV. The protein fractions collected were analyzed by 12 % SDS-PAGE stained using
322 Coomassie blue. The fractions containing TupA were concentrated and loaded onto a Superdex 75

HR10/300 GL column (GE-Healthcare) equilibrated with 50 mM potassium phosphate buffer containing 150 mM NaCl. The fraction containing the pure protein was pooled, concentrated and stored at -80 °C until further use. All the steps, including cell collection, soluble extract preparation and purification procedure, were performed at 4 ºC and pH 7.6.

3.4. Extinction coefficient determination.

The extinction coefficient was determined by measuring the absorbance at 280 nm of a pure TupA protein sample quantified using the Bradford method [38] with bovine serum albumin as standard. UV-visible absorption spectrum was performed on a Shimadzu UV-2101PC split beam spectrophotometer using 1 cm optical path quarts cells. The value obtained was in agreement with the one determined using the bioinformatic tool ProtParam from the ExPASy portal [28].

3.5. Protein gel shift assay

TupA gel shift assays were performed following the protocol described by Rech *et al* [8]. Briefly, TupA protein samples (14 µM) were incubated with MoO_4^{2-}, WO_4^{2-}, SO_4^{2-}, PO_4^{3-}, and ClO_4^{-}, anions (140 µM) in 25 mM Tris-HCl (pH 7.5) buffer at room temperature for 25 min. Unbound anions were separated from TupA with a PD10 desalting column (GE HealthCare). Protein samples were mixed with 0.25 volume of sucrose solution (30 % w/v) containing bromophenol blue and resolved on a native 12% polyacrylamide gel buffered with 50 mM Tris-HCl (pH 8.5). The electrophoresis was carried out at 100 V, 100 A and 4 °C using a 0.1 M Tris-HCl and 0.1 M glycine (pH 8.3) running buffer. The mobility shift assay after anion binding was visualized through the staining of the gel with Coomassie Blue staining solution.

3.6. Isothermal titration calorimetry

Isothermal titration calorimetry experiments were performed using a VP-ITC calorimeter (MicroCal GE Healthcare). Prior to experiments, protein was dialysed extensively against the reaction buffer (5 mM Tris-HCl (pH 7.5) made with Milli-Q dH2O). Binding protein (10 µM) was equilibrated in reaction buffer at 30 °C in the cell of the calorimeter and subsequently, 20 or 23 injections of 10 µl of a 100 µM sodium tungstate or molybdate solution were performed and the heat response recorded. After subtraction of the baseline, the integrated heats were fitted to the single binding site model using the ORIGIN software package supplied with the calorimeter. For competition experiments, the reaction buffer was supplemented with the stated concentrations of molybdate prior to the injections with sodium, tungstate or the reverse. The relationship between apparent dissociation constants and the underlying constants are derived from equation 1:

$$K_{app} = \frac{K_A}{(1+K_B[B])} \text{ (Eq1) [39]}$$

where K_A is the binding constant for the strong binding ligand and K_B is that for the competitively inhibiting ligand. The apparent binding constant depends on the concentration of the free competitively inhibiting ligand [B] [39].

3.7. Crystallization

TupA protein was concentrated up to 7.5 mg/ml in 5 mM Tris-HCl (pH 7.5) with a Vivaspin 20 ultrafiltration device (Sartorius Stedim Biotech S.A.). The final concentration of TupA was determined from the absorbance at 280 nm, using an extinction coefficient of 30440 M^{-1} cm^{-1}.
The first crystallization trials were performed at 20 ºC using the sitting-drop vapour diffusion method, with 0.5 µL of protein: 0.5 µL of precipitant solution on 96 well crystallization plates (SWISSCI 'MRC' 2-Drop Crystallization Plates, Douglas Instruments). Several commercial screens were used, namely the PEG/Ion HT (Hampton Research), the JBScreen Classic 1-10 (Jena Bioscience), and an 80 conditions in-house screen (based on the screen of Jancarik *et al.* [40]). The TupA crystallized in only one of the conditions of the in-house screen containing 0.2 M magnesium chloride, 0.1 M Hepes (pH 7.5) and 30 % (w/v) polyethylene glycol 3350. Colourless plate shaped crystals appeared within 4 days (Figure 6).
Scale-up and optimization experiments were performed and new crystals with maximum dimensions of 0.3x0.15x0.06 mm^3 appeared in hanging-drops with 2 µL of protein (at 7.5 mg/mL): 1 µL of precipitant solution on a 24 well crystallization plate. These crystals were used to for data collection.

3.7. Data collection and processing

The crystals were flash-cooled directly in liquid nitrogen, using paratone as cryoprotectant and maintained under a stream of nitrogen gas during data collection.
A complete dataset was collected at beamline ID23-1 at the European Synchrotron Radiation Facility (ESRF, Grenoble, France) and the crystal diffracted up to 1.43 Å at a wavelength of 0.954 Å. The TupA crystal belongs to the monoclinic space group $P2_1$ with the unit-cell parameters: a= 52.25 Å, b= 42.50 Å, c= 54.71 Å and β= 95.43˚. Matthews coefficient was calculated (ca 2.09 $Å^3$/Da) [41] suggesting the presence of one monomer (α) per asymmetric unit, with a solvent content of 40.84%.
Data was processed with XDS package [42] and AIMLESS [43] from the CCP4 program package v. 6.3.0 (Collaborative Computational Project, Number 4, 1994) [44]. The data collection and processing statistics are presented in the Table 2.

4. Conclusions

Transport of tungstate and other analogous oxoanions like molybdate is very relevant in organisms that contain key metabolic W/Mo-enzymes like *Desulfovibrio* species. Despite of this, there are no reports about characterization of molybdate/tungstate uptake systems from these SRB. Analysis of *Desulfovibrio* genome annotated to date show that molybdate and tungstate transporters are encoded in the chromosome of these organisms and belong to the Mod and Tup family of proteins, respectively [1]. Although Mo and W have similar biochemistry [45], molybdate and tungstate transporters can

differentiate between them. The molecular basis of the selectivity by the Tup and Mod transporters remain to be understood. Valuable information can be derived from the biochemical and structural characterization of the TupA protein and particularly from organisms that contain both (Mod and Tup) kind of transporters. In this work we report the expression, purification, preliminary characterization, crystallization and structure determination of *Da*G20 TupA. In order to attest the binding of molybdate and tungstate to *Da*G20 TupA gel shift assays were also carried out. Different from the TupA from *Eubacterium acidaminophilum* [9], *Da*G20 TupA not only efficiently binds tungstate but also molybdate anions. In order to quantitatively determine the binding affinity of TupA towards the two oxoanions, isothermal titration calorimetry was carried out. The obtained data show that TupA binds in a 1:1 stoichiometry the two anions but has much higher affinity to tungstate than to molybdate (around 1000 times lower K_D value for tungstate anions). Furthermore, in a competitive binding assay, the protein is capable of displacing the molybdate in order to bind what we think is its physiological partner, tungstate. In order to understand the specificity of TupA, site directed mutagenesis is under way where some of the putative key residues for binding are going to be inspected.

Conditions to crystallize TupA were found and the crystals diffracts up to 1.43 Å. The high resolution structure will allow detailed characterization of the ligand pocket, coordination geometry and conformational changes upon metal binding which will help to better understand the mode of action of these transporters.

Acknowledgments

This work was supported by Fundação para a Ciência e Tecnologia (EXPL/BBB-BEP/0274/2012). ARO-C, RRN and MASC thank FCT for grants (Reference SFRH/BD/85806/2012, SFRH/BPD/63061/2009 and SFRH/BPD/64917/2009). MGR is a member of the CONICET (Argentina).

The data collection was performed on the ID23-1 beamline at the European Synchrotron Radiation Facility (ESRF), Grenoble, France. We are grateful to Local Contact Christoph Mueller Dieckmann at ESRF for providing beamline assistance.

We acknowledge Faculdade de Medicina Veterinária da Universidade Técnica de Lisboa for the Isothermal titration calorimetry facility.

Author Contributions

Ana R Otrelo-Cardoso and Teresa Santos-Silva performed crystallization, data collection and processing experiments. Rashmi R Nair and Maria G Rivas cloned and optimized/purified TupA. Rashmi R Nair performed TupA preliminary characterization. Márcia A S Correia performed ITC experiments and data analysis. All the authors contributed to the preparation of the manuscript.

References and Notes

1. Gonzalez, P. J.; Rivas, M. G.; Mota, C. S.; Brondino, C. D.; Moura, I.; Moura, J. J. G., Periplasmic nitrate reductases and formate dehydrogenases: Biological control of the chemical properties of Mo and W for fine tuning of reactivity, substrate specificity and metabolic role. *Coord. Chem. Rev.* **2013,** 257, (2), 315-331.

2. Hagen, W. R., Cellular uptake of molybdenum and tungsten. *Coord. Chem. Rev.* **2011,** 255, (9–10), 1117-1128.

3. Schwarz, G.; Mendel, R. R.; Ribbe, M. W., Molybdenum cofactors, enzymes and pathways. *Nature* **2009,** 460, (7257), 839-847.

4. Grunden, A. M.; Shanmugam, K. T., Molybdate transport and regulation in bacteria. *Arch. Microbiol.* **1997,** 168, (5), 345-354.

5. Maupin-Furlow, J. A.; Rosentel, J. K.; Lee, J. H.; Deppenmeier, U.; Gunsalus, R. P.; Shanmugam, K. T., Genetic analysis of the modABCD (molybdate transport) operon of *Escherichia coli*. *J. Bacteriol.* **1995,** 177, (17), 4851-4856.

6. Rech, S.; Deppenmeier, U.; Gunsalus, R. P., Regulation of the molybdate transport operon, modABCD, of *Escherichia coli i*n response to molybdate availability. *J. Bacteriol.* **1995,** 177, (4), 1023-1029.

7. Anderson, L. A.; Palmer, T.; Price, N. C.; Bornemann, S.; Boxer, D. H.; Pau, R. N., Characterisation of the molybdenum-responsive ModE regulatory protein and its binding to the promoter region of the modABCD (molybdenum transport) operon of *Escherichia coli*. *Eur. J. Biochem.* **1997,** 246, (1), 119-126.

8. Rech, S.; Wolin, C.; Gunsalus, R. P., Properties of the periplasmic ModA molybdate-binding protein of *Escherichia coli*. *J. Biol. Chem.* **1996,** 271, (5), 2557-2562.

9. Makdessi, K.; Andreesen, J. R.; Pich, A., Tungstate uptake by a highly specific ABC transporter in *Eubacterium acidaminophilum*. *J. Biol. Chem.* **2001,** 276, (27), 24557-24564.

10. Bevers, L. E.; Hagedoorn, P. L.; Krijger, G. C.; Hagen, W. R., Tungsten transport protein A (WtpA) in *Pyrococcus furiosus*: the first member of a new class of tungstate and molybdate transporters. *J. Bacteriol.* **2006,** 188, (18), 6498-64505.

11. Imperial, J.; Hadi, M.; Amy, N. K., Molybdate binding by ModA, the periplasmic component of the *Escherichia coli* mod molybdate transport system. *Biochim. Biophys. Acta* **1998,** 1370, (2), 337-346.

12. Smart, J. P.; Cliff, M. J.; Kelly, D. J., A role for tungsten in the biology of *Campylobacter jejuni*: tungstate stimulates formate dehydrogenase activity and is transported via an ultra-high affinity ABC system distinct from the molybdate transporter. *Mol. Microbiol.* **2009,** 74, (3), 742-757.

13. Balan, A.; Santacruz, C. P.; Moutran, A.; Ferreira, R. C.; Medrano, F. J.; Perez, C. A.; Ramos, C. H.; Ferreira, L. C., The molybdate-binding protein (ModA) of the plant pathogen *Xanthomonas axonopodis* pv. citri. *Protein Expr. Purif.* **2006,** 50, (2), 215-222.

14. Taveirne, M. E.; Sikes, M. L.; Olson, J. W., Molybdenum and tungsten in *Campylobacter jejuni*: their physiological role and identification of separate transporters regulated by a single ModE-like protein. *Mol. Microbiol.* **2009,** 74, (3), 758-771.

15. Bevers, L. E.; Schwarz, G.; Hagen, W. R., A molecular basis for tungstate selectivity in prokaryotic ABC transport systems. *J. Bacteriol.* **2011,** 193, (18), 4999-5001.

16. Andreesen, J. R.; Makdessi, K., Tungsten, the surprisingly positively acting heavy metal element for prokaryotes. *Ann. N. Y. Acad. Sci.* **2008,** 1125, 215-29.

17. Hu, Y.; Rech, S.; Gunsalus, R. P.; Rees, D. C., Crystal structure of the molybdate binding protein ModA. *Nat. Struct. Biol.* **1997,** 4, (9), 703-707.

18. Lawson, D. M.; Williams, C. E.; Mitchenall, L. A.; Pau, R. N., Ligand size is a major determinant of specificity in periplasmic oxyanion-binding proteins: the 1.2 A resolution crystal structure of *Azotobacter vinelandii* ModA. *Structure* **1998,** 6, (12), 1529-1539.

19. Balan, A.; Santacruz-Perez, C.; Moutran, A.; Ferreira, L. C.; Neshich, G.; Goncalves Barbosa, J. A., Crystallographic structure and substrate-binding interactions of the molybdate-binding protein of the phytopathogen *Xanthomonas axonopodis* pv. citri. *Biochim. Biophys. Acta* **2008,** 1784, (2), 393-399.

20. Hollenstein, K.; Comellas-Bigler, M.; Bevers, L. E.; Feiters, M. C.; Meyer-Klaucke, W.; Hagedoorn, P. L.; Locher, K. P., Distorted octahedral coordination of tungstate in a subfamily of specific binding proteins. *J. Biol. Inorg. Chem.* **2009,** 14, (5), 663-672.

21. Feio, M. J.; Zinkevich, V.; Beech, I. B.; Llobet-Brossa, E.; Eaton, P.; Schmitt, J.; Guezennec, J., *Desulfovibrio alaskensis* sp. nov., a sulphate-reducing bacterium from a soured oil reservoir. *Int. J. Syst. Evol. Microbiol.* **2004,** 54, (5), 1747-1752.

22. Lee, W.; Lewandowski, Z.; Nielsen, P. H.; Hamilton, W. A., Role of sulfate-reducing bacteria in corrosion of mild-steel - a review. *Biofouling* **1995,** 8, (3), 165-168.

23. Hamilton, W. A., Microbially influenced corrosion as a model system for the study of metal microbe interactions: a unifying electron transfer hypothesis. *Biofouling* **2003,** 19, (1), 65-76.

24. Sanders, P. F.; Sturman, P. J., Biofouling in the oil industry. In *Petroleum Microbiology*, Olivier, B.; Magot, M., Eds. Washington, DC, 2005; pp 171-198.

25. Peck, H. D., The ATP-dependent reduction of sulfate with hydrogen in extracts of *Desulfovibrio desulfuricans*. *Proc. Natl. Acad. Sci. U S A* **1959,** 45, (5), 701-708.

26. Peck, H. D., Jr., Enzymatic basis for assimilatory and dissimilatory sulfate reduction. *J. Bacteriol.* **1961,** 82, 933-939.

27. Biswas, K. C.; Woodards, N. A.; Xu, H.; Barton, L. L., Reduction of molybdate by sulfate-reducing bacteria. *Biometals* **2009,** 22, (1), 131-139.

28. Gasteiger, E.; Hoogland, C.; Gattiker, A.; Duvaud, S.; Wilkins, M. R.; Appel, R. D.; Bairoch, A., Protein identification and analysis tools on the ExPASy Server;. In *The Proteomics Protocols Handbook*, Walker, J. M., Ed. Humana Press: 2005; pp 571-607.

29. Thompson, J. D.; Gibson, T. J.; Higgins, D. G., Multiple Sequence Alignment Using ClustalW and ClustalX. In *Current Protocols in Bioinformatics*, John Wiley & Sons, Inc.: 2002.

510 30. Padilla, J. E.; Yeates, T. O., A statistic for local intensity differences: robustness to anisotropy
511 and pseudo-centering and utility for detecting twinning. *Acta Crystallogr. D Biol. Crystallogr.*
512 **2003,** 59, (Pt 7), 1124-1130.

513 31. McCoy, A. J.; Grosse-Kunstleve, R. W.; Adams, P. D.; Winn, M. D.; Storoni, L. C.; Read, R.
514 J., Phaser crystallographic software. *J. Appl. Crystallogr.* **2007,** 40, (Pt 4), 658-674.

515 32. Postgate, J., In *The sulphate-reducing bacteria*, 2nd ed.; Cambridge University Press: London,
516 United Kingdom, 1984; pp 24-40.

517 33. Hauser, L. J.; Land, M. L.; Brown, S. D.; Larimer, F.; Keller, K. L.; Rapp-Giles, B. J.; Price,
518 M. N.; Lin, M.; Bruce, D. C.; Detter, J. C.; Tapia, R.; Han, C. S.; Goodwin, L. A.; Cheng, J.-F.;
519 Pitluck, S.; Copeland, A.; Lucas, S.; Nolan, M.; Lapidus, A. L.; Palumbo, A. V.; Wall, J. D.,
520 Complete genome sequence and updated annotation of *Desulfovibrio alaskensis* G20. *J.*
521 *Bacteriol.* **2011,** 193, (16), 4268-4269.

522 34. Wall, J. D.; Rapp-Giles, B. J.; Rousset, M., Characterization of a small plasmid from
523 *Desulfovibrio desulfuricans* and its use for shuttle vector construction. *J. Bacteriol.* **1993,** 175,
524 (13), 4121-4128.

525 35. Studier, F. W.; Moffatt, B. A., Use of bacteriophage T7 RNA polymerase to direct selective
526 high-level expression of cloned genes. *J. Mol. Biol.* **1986,** 189, (1), 113-130.

527 36. Altschul, S. F.; Lipman, D. J., Protein database searches for multiple alignments. *Proc. Nat.*
528 *Acad. Sci.* **1990,** 87, (14), 5509-5513.

529 37. Thompson, J. D.; Higgins, D. G.; Gibson, T. J., CLUSTAL W: improving the sensitivity of
530 progressive multiple sequence alignment through sequence weighting, position-specific gap
531 penalties and weight matrix choice. *Nucleic Acids Res.* **1994,** 22, (22), 4673-4680.

532 38. Bradford, M. M., A rapid and sensitive method for the quantitation of microgram quantities of
533 protein utilizing the principle of protein-dye binding. *Anal. Biochem.* **1976,** 72, 248-254.

534 39. Velazquez-Campoy, A.; Freire, E., Isothermal titration calorimetry to determine association
535 constants for high-affinity ligands. *Nat. Protoc.* **2006,** 1, (1), 186-191.

536 40. Jancarik, J.; Kim, S.-H., Sparse matrix sampling: a screening method for crystallization of
537 proteins. *J. Appl. Cryst.* **1991,** 24, (4), 409-411.

538 41. Matthews, B. W., Solvent content of protein crystals. *J. Mol. Biol.* **1968,** 33, (2), 491-497.

539 42. Kabsch, W., Xds. *Acta Crystallogr. D Biol. Crystallogr.* **2010,** 66, (Pt 2), 125-132.

540 43. Evans, P., Scaling and assessment of data quality. *Acta Crystallogr. D Biol. Crystallogr.* **2006,**
541 62, (1), 72-82.

542 44. The CCP4 suite: programs for protein crystallography. *Acta Crystallogr. D Biol. Crystallogr.*
543 **1994,** 50, (Pt 5), 760-763.

544 45. Bevers, L. E.; Hagedoorn, P.-L.; Hagen, W. R., The bioinorganic chemistry of tungsten. *Coord.*
545 *Chem. Rev.* **2009,** 253, (3–4), 269-290.

546